

# Resource Requirements for Fault-Tolerant Quantum Simulation: The Transverse Ising Model Ground State

Craig R. Clark<sup>1</sup>, Tzvetan S. Metodi<sup>2</sup>, Samuel D. Gasster<sup>2</sup>, and Kenneth R. Brown<sup>1\*</sup>

<sup>1</sup>*School of Chemistry and Biochemistry and Division of Computational Science and Engineering,  
Georgia Institute of Technology, Atlanta, GA 30332-0400 and*

<sup>2</sup>*Computer Systems Research Department, The Aerospace Corporation, El Segundo, CA 90245-4691*

(Dated: September 11, 2018)

We estimate the resource requirements, the total number of physical qubits and computational time, required to compute the ground state energy of a 1-D quantum Transverse Ising Model (TIM) of  $N$  spin-1/2 particles, as a function of the system size and the numerical precision. This estimate is based on analyzing the impact of fault-tolerant quantum error correction in the context of the Quantum Logic Array (QLA) architecture. Our results show that due to the exponential scaling of the computational time with the desired precision of the energy, significant amount of error correction is required to implement the TIM problem. Comparison of our results to the resource requirements for a fault-tolerant implementation of Shor's quantum factoring algorithm reveals that the required logical qubit reliability is similar for both the TIM problem and the factoring problem.

## I. INTRODUCTION

The calculation of the basic properties of quantum systems (eigenstates and eigenvalues) remains a challenging problem for computational science. One of the most significant issues is the exponential scaling of the computational resource requirements with the number of particles and degrees of freedom, which for even a small number of particles ( $\sim 100$ ) exceeds the capabilities of current computer systems. In 1982 Feynman addressed this problem by proposing that it may be possible to use one quantum system as the basis for the simulation of another [1]. This was the early promise of quantum simulation, and one of the original motivations for quantum computing. Since that time, many researchers have investigated different approaches to quantum simulation [2, 3, 4, 5, 6, 7]. For example, Abrams and Lloyd have proposed a quantum algorithm for the efficient computation of eigenvalues and eigenvectors using a quantum computer [4]. Many of the investigations into quantum simulation have assumed ideal performance from the underlying components resulting in optimistic estimates for the quantum computer resource requirements (number of

---

\*Electronic address: ken.brown@chemistry.gatech.edu

qubits and time to completion). It is well known, however, that in order to address the effects of decoherence and other sources of faults and errors in the implementation of qubits and gates it is necessary to incorporate fault-tolerant quantum error correction into an estimate of the resource requirements.

In this paper we estimate the resource requirements for a quantum simulation of the ground state energy for the 1-D quantum Transverse Ising Model, specifically incorporating the impact of fault-tolerant quantum error correction. We apply the general approach of Abrams and Lloyd [3, 4], and compute estimates for the total number of physical qubits and computational time as a function of the number of particles ( $N$ ) and required numerical precision ( $M$ ) in the estimate of the ground state energy.

We have chosen to study the resource requirements for computing the ground state energy for the 1-D quantum TIM since this model is well studied in the literature and has an analytical solution [8, 9, 10]. The relevant details of the TIM are summarized in Section II. In Section III, we map the calculation of the TIM ground state energy onto a quantum phase estimation circuit that includes the effects of fault-tolerant quantum error correction. The required unitary transformations are decomposed into one qubit gates and two-qubit controlled-not gates using gate identities and the Trotter formula. The one-qubit gates are approximated by a set of gates which can be executed fault-tolerantly using the Solovay-Kitaev theorem [11]. In Section III C, the quantum circuit is mapped onto the Quantum Logic Array (QLA) architecture model, previously described by Metodi, et al. [12]. Our final results, utilizing the QLA architecture, are given in Section III D and a discussion of how improving the state of the art in the underlying technology affects the performance for executing the TIM problem. In Section IV, we extend our resource estimate from 1-D to higher dimensions. Since the QLA architecture was developed to study the fault-tolerant resource requirements for Shor's quantum factoring algorithm [13], we compare our present results for the TIM quantum simulation with previous analysis of the the resource requirements for Shor's algorithm, in Section V. Finally, our conclusions are presented in Section VI.

## II. TRANSVERSE ISING MODEL

The 1-D Transverse Ising Model is one of the simplest models exhibiting a quantum phase transition at zero temperature [8, 9, 14, 15]. The calculation of the ground state energy of the TIM varies from analytically solvable in the linear case [8] to computationally inefficient for frustrated 2-D lattices [16]. For example, the calculation of the magnetic behavior of frustrated Ising antiferromagnets requires computationally intensive Monte-Carlo simulations [17]. Given the difficulty of the generic problem and the

centrality of the TIM to studies of quantum phase transitions and quantum annealing, the TIM is a good benchmark model for quantum computation studies.

The 1-D Transverse Ising Model consists of  $N$ -spin-1/2 particles at each site of a one dimensional linear lattice (with the spin axis along the  $z$ -axis) in an external magnetic field along to  $x$ -axis. The Hamiltonian for this system,  $H_I$ , may be written as [9]:

$$H_I = \sum_i \Gamma \sigma_i^x + \sum_{\langle i,j \rangle} J_{ij} \sigma_i^z \sigma_j^z, \quad (1)$$

where  $J$  is the spin-spin interaction energy,  $\Gamma$  is the coupling constant and related to the strength of the external magnetic field along the  $\hat{x}$ -direction, and  $\langle i, j \rangle$  implies a sum only over nearest-neighbors.  $\sigma_i^x$  and  $\sigma_i^z$  are the Pauli spin operators for the  $i$ th spin, and we set  $\hbar = 1$  throughout this paper.

In present work we focus is on the 1-D linear chain TIM of  $N$ -spins with constant Ising interaction energy  $J_{ij} = -J$ . The ground state of the system is determined by the ratio of  $g = \Gamma/J$ . For the large magnetic field case,  $g \gg 1$  the system is paramagnetic with all the spins aligned along the  $\hat{x}$  axis, and in the limit of small magnetic field,  $g \ll 1$ , the system has two degenerate ferromagnetic ground states, parallel and anti-parallel to the  $\hat{z}$  axis. In the intermediate range of magnetic field strength the linear 1-D TIM exhibits a quantum phase transition at  $g = 1$  [9].

The TIM Hamiltonian in Equation 1, for the 1-D case with constant coupling can be rewritten as:

$$H_I = -J \left( \sum_{j=1}^N g X_j + \sum_{j=1}^{N-1} Z_j Z_{j+1} \right) \quad (2)$$

where the Pauli spin operators are replaced with their corresponding matrix operators  $X_j, Z_j$ . For the 1-D TIM, the ground state energy can be calculated analytically in the limit of large  $N$ [8]. In the case of a finite number of spins with non-uniform spin-spin interactions ( $J$  not constant), it is possible to efficiently simulate the TIM using either the Monte-Carlo method [18] or the density matrix renormalization group approach [10]. The challenge for classical computers comes from the 2-D TIM on a frustrated lattice where the simulation scales exponentially with  $N$ . Applying the quantum phase estimation circuit to calculate the ground state energy of the TIM requires physical qubit resources, which scale polynomially with  $N$ , and the number of computational time steps is also polynomial in  $N$ . In addition, just as the complexity of the problem is independent of the lattice dimension and layout when applying classical brute force diagonalization, the amount of resources required to apply the quantum phase estimation circuit is largely independent of the dimensionality of the TIM Hamiltonian.

### III. TIM QUANTUM SIMULATION RESOURCE ESTIMATES

Our approach to estimating the resource requirements for the TIM ground-state energy calculation with Hamiltonian  $H_I$  involves two steps. First, we follow the approach of Abrams and Lloyd and map the problem of computing the eigenvalues of the TIM Hamiltonian in Equation 2 onto a phase estimation quantum circuit [3, 4]. Second, we decompose each operation in the phase estimation circuit into a set of universal gates that can be implemented fault-tolerantly within the context of the QLA architecture. This allows us an accurate estimate of the resources in a fault-tolerant environment.

#### A. Phase estimation circuit

The phase estimation algorithm allows one to calculate an  $M$ -bit estimate of the phase  $\phi$  of the eigenvalue  $e^{-i2\pi\phi}$  of the time evolution unitary operator  $U(\tau) = e^{-iH_I\tau}$ , where the time  $\tau$  is constant throughout the implementation of the phase estimation algorithm. The desired energy eigenvalue  $E$  of  $H_I$  can be computed using  $\phi$  by calculating  $E = \frac{2\pi\phi}{\tau}$ .

The value of  $\tau$  is determined by the fact that the output from the phase estimation algorithm is the binary fraction  $0.x_1 \dots x_M$ , which is less than one [3, 4]. In order to ensure that this result is a valid approximation of the phase  $\phi$ , we must set the parameter  $\tau$  such that  $\tau < 2\pi/E$ , which corresponds to  $\phi < 1$ . For the 1-D TIM, the magnitude of the ground-state energy  $|E_g|$  is bounded by  $NJ(1+g)$  [8]. In the region near the phase transition  $g \approx 1$ , we choose  $\tau = (10JN)^{-1}$ , which satisfies  $\tau < 2\pi/|E_g|$ .

The quantum circuit for implementing the phase estimation algorithm is shown in Figure 1. The circuit consists of two quantum registers: an  $N$ -qubit input quantum register prepared in an initial quantum state  $|\Psi\rangle$ , and an output quantum register consisting of a single qubit recycled  $M$  times [19, 20]. Each of the  $N$  qubits in the input register corresponds to one of the  $N$  spin-1/2 particles in the TIM model [21]. At the beginning of each of the  $M$  steps in the algorithm, the output qubit is prepared into the state  $\frac{1}{\sqrt{2}}(|0\rangle + |1\rangle)$  using a Hadamard (H) gate. The H gate is followed by a controlled power of  $U(\tau)$ , denoted with  $U(2^m\tau)$ , applied on the input register, where  $0 \leq m \leq M-1$ .

Letting  $j$  denote to the  $j$ th step in the circuit, each time the output qubit is measured (meter symbols) the result is in the  $m$ th bit in the estimate of  $\phi$ , following the rotation of the output qubit via the gate:

$$R_j = |0\rangle\langle 0| + \exp\left(i\pi \sum_{m=M+2-j}^M \frac{2^{M+1}x_m}{2^{m+j}}\right) |1\rangle\langle 1| \quad (3)$$

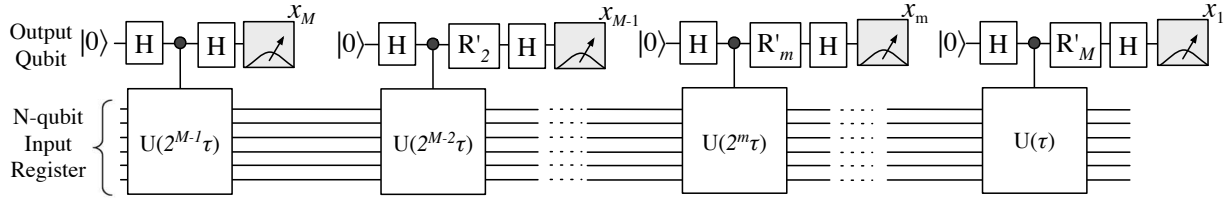


FIG. 1: The circuit for implementing the phase estimation algorithm using one continuously recycled control qubit.

where the gate  $R_j$  corresponds to the application of the Quantum Fourier Transform on the output qubit at each step [19, 20]. The result after each of the  $M$  measurements is an  $M$ -bit binary string  $\{x_1 x_2 \dots x_M\}$ , which corresponds the  $M$ -bit approximation of  $\phi$  given by  $0.x_1 \dots x_M$ . Using this estimate of  $\phi$ , the corresponding energy eigenvalue  $E = \frac{2\pi\phi}{\tau}$  will be the ground-state energy  $E_g$  with probability equal to  $|\langle\Psi|\Psi_g\rangle|^2$  [3], where  $|\Psi_g\rangle$  is the ground eigenstate of  $H_I$ .

To maximize the probability of success  $|\langle\Psi|\Psi_g\rangle|^2$ , the initial quantum state  $|\Psi\rangle$  should be an approximation of the ground state  $|\Psi_g\rangle$ . For arbitrary Hamiltonians the preparation of an approximation to  $|\Psi_g\rangle$  is generally computationally difficult [22, 23]. For certain cases, the preparation can be accomplished using classical approximation techniques to calculate an estimated wavefunction or adiabatic quantum state preparation techniques [6, 21]. If the state can be prepared adiabatically, the resource requirements for preparing  $|\Psi\rangle$  are comparable in complexity to the resource requirements for implementing the circuit for the phase estimation algorithm shown in Figure 1 [21]. For this reason, we focus our analysis on estimating the number of computational time steps and qubits required to implement the circuit, assuming that the input register has been already prepared into the  $N$ -qubit quantum state  $|\Psi\rangle$ .

### B. Decomposition of the TIM quantum circuit into fault-tolerant gates

Figure 1 in Section III A shows the TIM circuit at a high-level, involving  $N + 1$  unitary operators. In this section, each unitary operation of the circuit is decomposed into a set of basic one and two qubit gates which can be implemented fault-tolerantly using the QLA architecture. The set of basic gates used is

$$\{X, Z, H, T, S, \text{CNOT}, \text{MEASURE}\} \quad (4)$$

where  $\text{MEASURE}$  is a single qubit measurement in the  $\hat{z}$  basis,  $\text{CNOT}$  denotes the two-qubit controlled-NOT gate, and  $T$  and  $S$  gates are single-qubit rotations around the  $\hat{z}$ -axis by  $\pi/4$  and  $\pi/2$  radians respectively. The high-level circuit operations which require decomposition are the controlled- $U(2^m \tau)$  gates and each  $R_j$  gate.

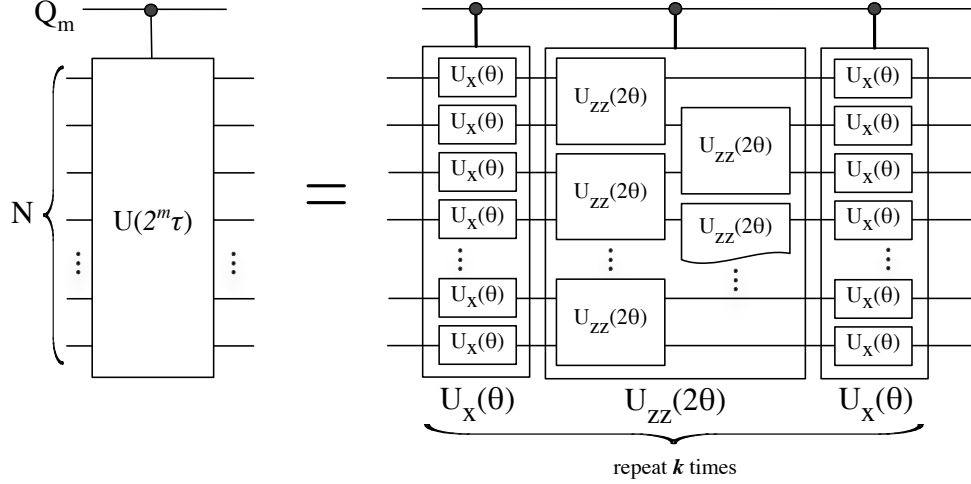


FIG. 2: Circuit for the controlled unitary operation  $U(2^m \tau)$  approximated using the Trotter formula.

The Controlled- $U(2^m \tau)$  gate can be decomposed using the second-order Trotter formula [24, 25]. First,  $H_I$  is broken into two terms:  $H_X = \sum_{j=0}^N gX_j$ , representing the transverse magnetic field, and  $H_{ZZ} = \sum_{j=0}^{N-1} Z_j Z_{j+1}$ , representing the Ising interactions. By considering the related unitary operators

$$U_x(2\tau) = \prod_{j=1}^N \exp(-ig\tau X_j) \quad (5)$$

$$U_{zz}(2\tau) = \prod_{j=1}^{N-1} \exp(-i\tau Z_j Z_{j+1}), \quad (6)$$

where we set  $g = 1$ , as discussed in Section II. We can construct the Trotter approximation of  $U(2^m \tau)$ , denoted by  $\tilde{U}(2^m \tau)$  as:

$$\begin{aligned} U(2^m \tau) &= [U_x(\theta) U_{zz}(2\theta) U_x(\theta)]^k + \epsilon_T \\ &= \tilde{U}(2^m \tau) + \epsilon_T, \end{aligned} \quad (7)$$

where  $\theta = (2^m \tau/k)$  and  $\epsilon_T$  is the Trotter approximation error, which scales as  $\mathcal{O}\left(\frac{(2^m \tau)^3}{k^2}\right)$  [24]. The Trotter approximation error can be made arbitrarily small by increasing the integer Trotter parameter  $k$ . Since the controlled- $U(2^m \tau)$  corresponds to the  $(M - m)$ th bit,  $\epsilon_T$  must be less than  $1/2^{M-m}$ , which is the precision of the  $(M - m)$ th measured bit in the binary fraction for the phase  $\phi$ . Thus, when approximating  $U(2^m \tau)$ ,  $k$  is increased until  $\epsilon_T$  is less than  $1/2^{M-m}$ . For a given  $M$ , we estimate a numerical value for the Trotter parameter  $k(m = 0) = k_0$  as a function of  $N \leq 10$ , with the constraint that  $\epsilon_T < 1/2^M$ . We thus find that for fixed  $M$ ,  $k_0$  scales as  $1/N$ . We use the exponent based on  $N \leq 10$  to extrapolate  $k_0$  for larger  $N$ . For  $m > 0$ , we set  $k = 2^m k_0$ , which will satisfy the error bound based on the scaling of  $\epsilon_T$  with  $k$ .

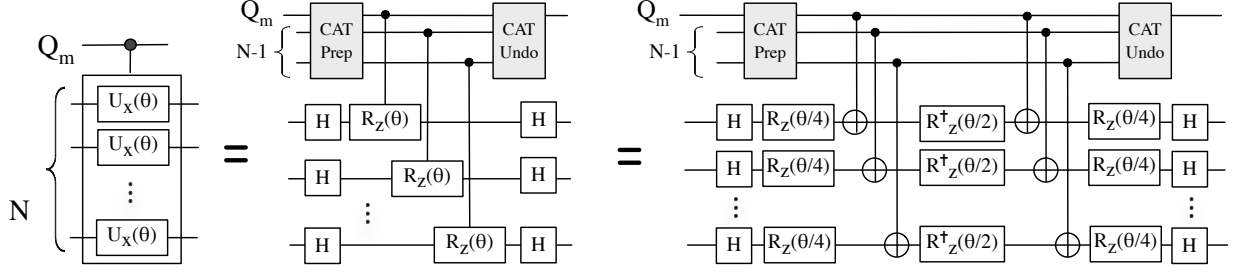


FIG. 3: The decomposition of the controlled unitary operation  $U_x(\theta)$  into single-qubit  $R_z$  gates and CNOT gates.

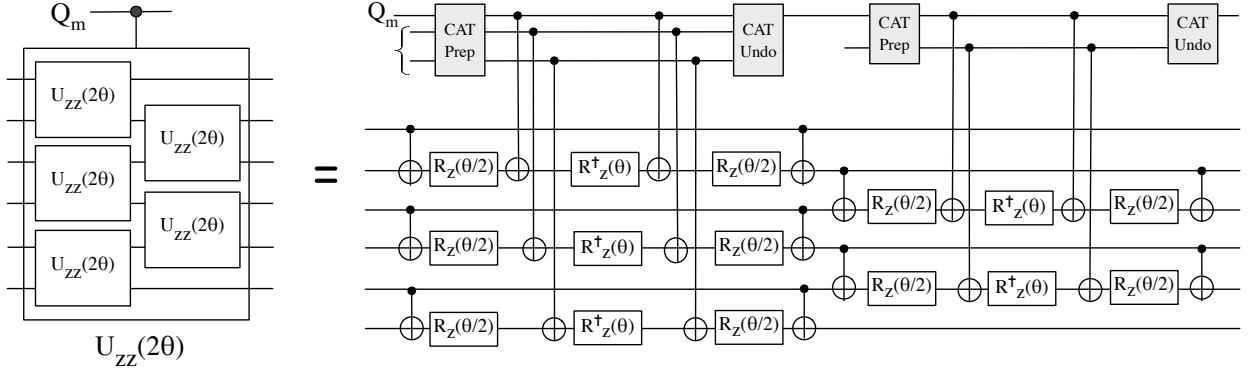


FIG. 4: The decomposition of the controlled unitary operation  $U_{zz}(2\theta)$  gate into single-qubit  $R_z$  gates and CNOT gates.

The circuit corresponding to the Trotter approximation of  $U(2^m\tau)$  is shown in Figure 2, where it can be seen that the controlled- $U(2^m\tau)$  is composed of two controlled- $U_x(\theta)$  operations and a controlled- $U_{zz}(\theta)$  operation, repeated  $k$  times and controlled on the  $m$ th instance of the output qubit denoted with  $Q_m$ . Expanding the circuit in Figure 2, we can express  $\tilde{U}(2^m\tau)$  as:

$$\tilde{U}(2^m\tau) = U_x(\theta) [U_{zz}(2\theta)U_x(2\theta)]^{k-1} U_{zz}(2\theta)U_x(\theta), \quad (8)$$

which shows that, approximating  $U(2^m\tau)$  will require the sequential implementation of  $k$  controlled- $U_{zz}(2\theta)$  gates,  $(k-1)$  controlled- $U_x(2\theta)$  gates, and two instances of controlled- $U_x(\theta)$  gates, all controlled on the  $m$ th instance of the output qubit.

The quantum circuits for the decomposition of the controlled- $U_x(2\theta)$  and controlled- $U_{zz}(2\theta)$  gates are shown in Figures 3 and 4, respectively. The gates are decomposed into rotations about the  $\hat{z}$ -axis,  $R_z(\theta) = \exp(-i\frac{\theta}{2}Z)$  and CNOT gates.  $(N-1)$  additional qubits are used to prepare an  $N$ -qubit cat state in order to parallelize each of the  $N$   $R_z(\theta)$  gates. The preparation of an  $N$ -qubit cat state requires  $(N-1)$  CNOT gates, which can be implemented in  $\mathcal{O}(N)$  time steps in parallel with the  $R_z(\theta/4)$  gates in Figure 3 and in parallel with the  $R_z(\theta/2)$  gates in Figure 4.

The three single-qubit  $R_z$  gates ( $R_z(\theta)$ ,  $R_z(\theta/2)$ , and  $R_z(\theta/4)$ ) can be approximated using  $\mathcal{O}(\log^{3.97}(1/\epsilon_{sk}))$  basic gates ( $H, T, S$ ) with the Solovay-Kitaev theorem [11, 26]. The Solovay-Kitaev error ( $\epsilon_{sk}$ ) is equivalent to a small rotation applied to the qubit. Using the results of Dawson and Nielsen [26] and  $\theta = \frac{2^m \tau}{k}$ , to compute the sequence of  $H, T$ , and  $S$  gates required to approximate each of the three  $R_z$  gates. We define  $S_R$  as the length of the longest of these three sequences. For  $M=30$ , for example, we find that  $S_R = 4 \times 10^5$ , requiring a sixth order [26] Solovay-Kitaev approximation. The results of this calculation show that the Solovay-Kitaev error  $\epsilon_{sk} < \frac{\epsilon_T}{k}$ , in order that the total error,  $\epsilon_T$  is less than the required precision ( $1/2^{M-m}$ ), when we approximate  $U(2^m \tau)$ . As a result  $S_R$  scales as  $\mathcal{O}(\log^{3.97}(k/\epsilon_T)) = \mathcal{O}(M^{3.97})$ .

We now have a complete decomposition of the controlled- $U(2^m \tau)$  into the basic gates given in Equation 4. As a function of  $S_R$ , the number of time steps required to implement controlled- $U_x(\theta)$  and  $U_{zz}(\theta)$  is equal to  $(3S_R + 4)$ , and  $(6S_R + 7)$ , respectively. Following Equation 8, the number of time steps required to implement the entire controlled- $U(2^m \tau)$  is  $k(9S_R + 11) + 3S_R + 4$ , where  $k = 2^m k_0$ . Each  $R_j$  gate in Figure 1 is equivalent to at most a rotation by  $R_z(\theta)$  and requires less than  $S_R$  gates.

Putting all of the above together, the total number of time steps ( $K$ ) required to implement the TIM circuit as a function of  $S_R, k_0$ , and  $M$  is given by:

$$\begin{aligned} K &= \sum_{m=0}^{M-1} [2^m k_0(9S_R + 11) + 3S_R + 4 + S_R] \\ &= \mathcal{O}(2^M) \times S_R, \quad (M \rightarrow \infty) \end{aligned} \quad (9)$$

Since  $S_R$  scales as  $\mathcal{O}(M^{3.97})$ , the total number of time steps is dominated by the exponential dependence on the precision ( $M$ ). The number of qubits  $Q$  required to implement the circuit is  $2N$ , since  $N$  qubits are needed for the input register  $|\Psi\rangle$ , one qubit is needed for the output register, and  $N - 1$  qubits are needed for the cat state.

In the next section we include fault-tolerant QEC into our circuit model and determine the resulting resource requirements,  $K$  and  $Q$ . We also provide an estimate on how long it could take to implement the TIM problem in real-time by taking into account the underlying physical implementation of each gate and qubit in the context of the QLA architecture.

### C. Mapping onto the QLA architecture

Incorporating quantum error correction and fault-tolerance [27, 28, 29, 30] into the TIM circuit design will impact the resource requirements in two ways. First, each of the qubits becomes a *logical qubit*, that is encoded into a state using a number of lower-level qubits. Second, each gate becomes a *logical gate*,

realized via a circuit composed of lower-level gates applied on the lower-level qubits that make-up a logical qubit. Each lower-level qubit may itself be a logical qubit all the way down to the physical level. Thus, quantum error correction and fault-tolerance increases the number of physical time steps and qubits required to implement each basic gate and may even require additional logical qubits, depending on how each gate is implemented fault-tolerantly and the choice of error correcting code. The resource requirements necessary to implement encoded logical qubits and gates will depend on the performance parameters of the underlying physical technology, the type of error correcting code used, and the level of reliability required per logical operation. The physical technology performance parameters that are taken into account in the design of the QLA architecture are the physical gate implementation reliability, time to execute a physical gate, and the time it takes for the state of the physical qubits to decohere.

The QLA architecture [12] is a tile-based, homogeneous quantum computer architecture based on ion trap technology, employing 2-D surface electrode trap structures [31, 32, 33]. Each tile represents a single computational unit capable of storing two logical qubits and executing fault-tolerantly any logical gate from the basic gate set given in Equation 4. One of the key features of the QLA architecture is the teleportation-based logical interconnect which enables logical qubit exchange between any two computational tiles. The interconnect uses the entanglement-swapping protocol [34] to enable logical qubit communication without adding any overhead to the number of time required to implement a quantum circuit [12].

The QLA was originally designed based on the requirement to factor 1024-bit integers [12]. This requirement resulted in the need to employ the second order concatenated Steane  $[[7, 1, 3]]$  quantum error correcting code [35]. Second order concatenation means that each logical qubit is a level 2 qubit, composed of 7 level 1 logical qubits each encoded into the state of 7 physical ion-trap qubits.

To estimate the reliability for executing each of the basic-gates fault-tolerantly, a lower-bound of  $3.1 \times 10^{-6}$  for the fault-tolerant threshold of the  $[[7, 1, 3]]$  code. This value was derived by Metodi, et al [36], by analysis of the ion-trap-based geometrical layout of each logical qubit tile. The  $[[7, 1, 3]]$  code threshold value used in the current research differs from the previously published estimate of  $1.8 \times 10^{-5}$  [37] due to our more detailed account of the operations specific to the ion trap technology in the implementation of each logical qubit [36]. Gottesman's methodology [38], which takes into account qubit movement, and these threshold results we estimate the reliability for each logical operation at levels 1 and 2.

Since each qubit in the  $[[7, 1, 3]]$  code moves an average of 10 steps during error correction [36], we find that each level 1 gate has a failure probability of  $3.2 \times 10^{-10}$  and each level 2 gate has a failure probability of  $3.5 \times 10^{-14}$ . In our failure probability estimates, we have assumed optimistic physical ion trap gate error probabilities of  $10^{-7}$  per physical operation, consistent with recent ion-trap literature [39]. We also

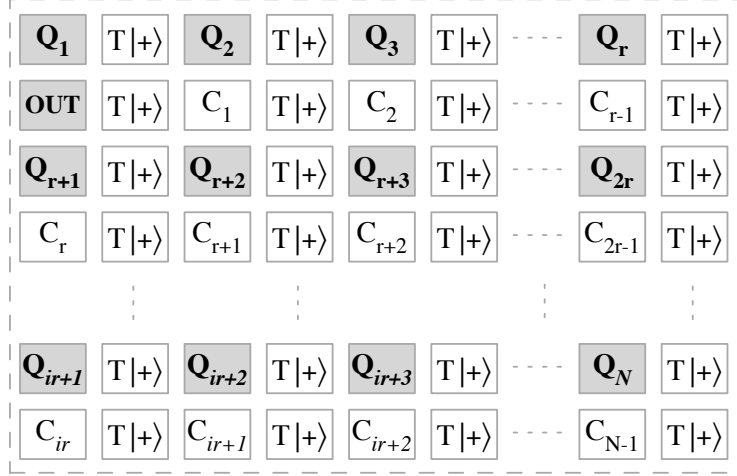


FIG. 5: QLA architecture for the TIM problem

determine the physical resources required for each logical qubit. Each level 1 qubit requires 21 ion-trap qubits (7 data qubits and 14 ancilla to facilitate error correction) and each level 2 qubit requires 21 level 1 qubits. Given that the duration of each physical operation on an ion-trap device is currently on the order  $10 \mu s$  [40, 41], the time required to complete a single error correction step is approximately 1.6 ms at level 1 and 0.26 seconds at level 2.

The number of logical qubits  $Q$  directly maps to the number of computational tiles required by the QLA, allowing us to estimate the size of the physical system. Similarly, the number of time steps  $K$  maps directly to the time required to implement the application since the duration of a single time step in the QLA architecture is defined as the time required to perform error correction, as discussed in Reference [12]. We define an aggregated metric  $KQ$  called the problem size equal to  $K \times Q$ , which is an upper bound on the total number of logical gates executed during the computation [42]. The inverse of the problem size,  $1/KQ$ , is the maximum failure probability allowed in the execution of a logical gate [42], which ensures that the algorithm completes execution at least 36% of the time. Taking into consideration the failure probabilities per logical gate, the maximum problem size  $KQ$  which can be implemented in the QLA architecture is  $3.1 \times 10^9$  at level 1 error correction,  $3 \times 10^{13}$  at level 2, and  $2.8 \times 10^{20}$  at level 3. Level 3 error correction is not described in the design of the QLA architecture, however, its implementation is possible since a level 3 qubit is simply a collection of level 2 qubits and the architecture design does not change. The estimated failure probability for each level 3 logical gate is  $3.6 \times 10^{-21}$ .

The parameters  $K$  and  $Q$  for the TIM problem were estimated in Section III B, where  $Q$  was found to be  $2N$  and  $K$  is on the order of  $\mathcal{O}(2^M) \times S_R$ . The fault-tolerant implementation of the  $T$  gate, however, requires an auxiliary logical qubit prepared into the state  $T|+\rangle$  for one time step followed by four time

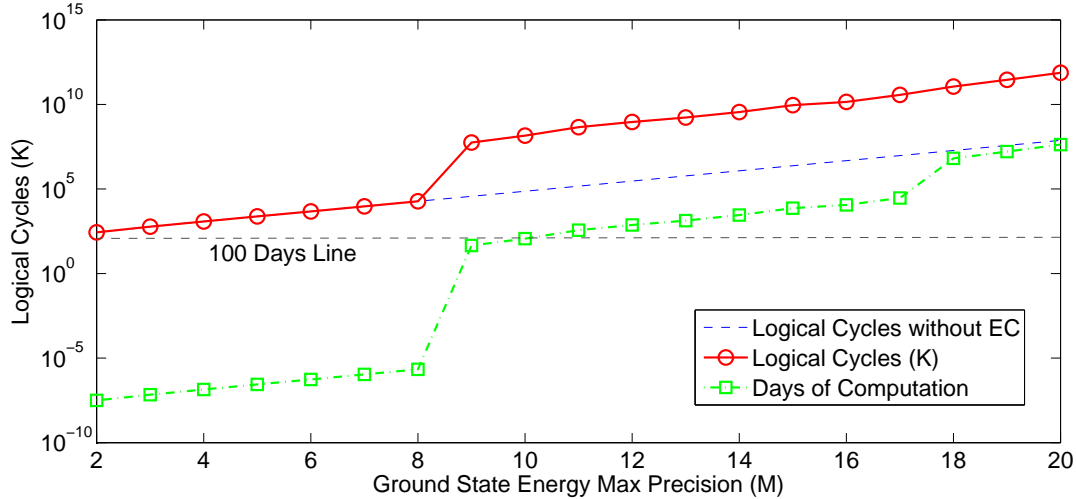


FIG. 6: (color online) Numerical calculations for the number of logical cycles  $K$  (solid line) and days of computation necessary assuming  $N = 100$  spin TIM problem as a function of the desired maximum precision  $M \leq 20$ .

steps composed of  $H$ , CNOT,  $S$ , and MEASURE gates [43], causing the value of  $K$  and  $Q$  to increase. Since many of the gates in the Solovay-Kitaev sequences approximating the  $R_z$  gates are  $T$  gates, when calculating  $K$  using Equation 9, the value of  $S_R$  must take into consideration the increased number of cycles for each  $T$  gate. All other basic gates are implemented transversally and require only one time step.

The resulting functional layout for the QLA architecture for the TIM problem is shown in Figure 5. The architecture consists of  $4N$  logical qubit tiles. The tiles labeled with  $Q_1$  through  $Q_N$  are the data tiles which hold the logical qubits used in the  $N$ -qubit input register  $|\Psi\rangle$  and the “OUT” tile is for the output register. The tiles labeled with  $C_1$  through  $C_{N-1}$  are the  $N - 1$  qubit tiles for the cat state. The  $T|+\rangle$  tiles are for the preparation of the auxiliary states in the event that  $T$  gates are applied on any of the data qubits. All tiles are specifically arranged as shown in Figure 5 in order to minimize the communication required for each logical CNOT gate between the control and target qubits. For example, when preparing the cat state using all  $C_i$  tiles and the “OUT” tile, CNOT gates are required only between the “OUT” tile,  $C_1$ , and  $C_r$ . Similarly,  $C_1$  interacts via a CNOT gate only with  $C_2$ , while  $C_2$  interacts only with  $Q_3$ , during the cat state preparation.

#### D. Resource estimates for the 1-D TIM problem

The resource requirements for implementing the 1-D TIM problem using the QLA architecture are given in Figure 6, where we show a logarithmic plot of the number of time steps  $K$  (calculated using Equation

9) as a function of the energy precision  $M \leq 20$ , assuming  $N = 100$ . The figure clearly shows  $K$ 's exponential dependence on  $M$ . The dependence of  $K$  on the number of spins ( $N$ ) is negligible and appears only in the  $k_0$  term in Equation 9 as  $\mathcal{O}(1/N)$ , as discussed in Section III B. In fact, since  $Q = 4N$ , we expect very little increase in the value of the total problem size  $KQ$  as  $N$  increases.

We see that for  $M \leq 8$  no error correction is required. This is because the required reliability per gate of  $1/KQ$  is still below the physical ion-trap gate reliability of  $1 \times 10^{-7}$ . Without error correction, the architecture is composed entirely of physical qubits and all gates are physical gates. This means that each single-qubit  $R_z$  gate can be implemented directly without the need to approximate it using the Solovay-Kitaev theorem, resulting in  $S_R = 1$  in Equation 9, and the total number of qubits becomes  $2N$  instead of  $4N$ . For  $M \geq 9$  error correction is required, resulting in a sudden jump in the number of timesteps at  $M = 9$ , with an additional scaling factor of  $\mathcal{O}(M^4)$  in  $K$  due to  $S_R$ 's dependence on  $M$ . In fact,  $K$  increases so quickly that at  $M = 9$  that level 2 error correction is required instead of level 1. At  $M \geq 18$  level 3 error correction is required and while there is no increase in  $K$ , each time step is much longer, so there is a jump in the number of days of computation. The Solovay-Kitaev order [26] for  $M = 9$  is three and increases to order five for  $M = 20$ .

### E. Discussion of the resource estimates

Our resource estimates for the 1-D TIM problem indicate that multiple levels of error correction, even for modest precision requirements, results in long computational times. As shown in Figure 6, it takes longer than 100 days, even for  $M = 7$ , when level 2 error correction is required. When level 3 error correction is required the estimated time is greater than  $7.5 \times 10^3$  years.

The number of logical cycles  $K$ , which grows exponentially with  $M$ , contributes to the long computational times. However, the primary factor contributing to the long computational time is the time it takes to implement a single logical gate using error correction. Presently, it is difficult to see how one might reduce the value of  $K$  short of implementing a different approach for solving quantum simulation problems. On the other hand, the logical gate time can be improved by implementing small changes in three parameters: decreasing the physical gate time  $t_p$ , increasing the threshold failure probability  $p_{th}$ , and decreasing the underlying physical failure probability  $p_0$ .

The effect of these three parameters on the overall computational time for the 1-D TIM problem is shown in Figure 7. The figure shows how the total time, in days, for  $M = 18$  varies as we improve each of the three parameters by a factor of 2 during each of the 10 iterations shown. The starting values for each

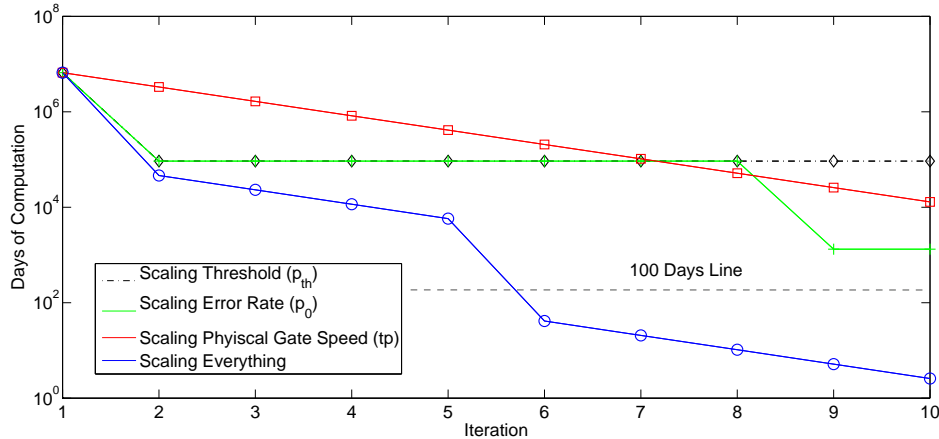


FIG. 7: (color online) The total computation time in days as we vary the physical cycle time  $t_p$  (square markers), physical failure probability  $p_0$  (starred markers), threshold failure probability  $p_{th}$  (diamond markers), and all together (circular markers) by a factor of two over 10 iterations.

parameter in the figure are  $3.1 \times 10^{-6}$  for  $p_{th}$ ,  $10^{-7}$  for  $p_0$  and  $10 \mu\text{s}$  for  $t_p$ . Decreasing the physical failure probability and increasing the threshold values by a factor of 2 during each iteration causes the number of days to decrease quadratically whenever lower error correction level is required, otherwise the number of days remains constant from one iteration to the next. A single change in the error correction level from level 3 to level 2 occurs by increasing  $p_{th}$  by a factor of 2 but there is no gain from additional increases in the threshold alone. Decreasing only  $p_0$  by a factor of 512 yields two changes in the error correction level.

From this analysis, we see that in order to reach a computational time on the order of 100 days with only level 1 error correction, we need to achieve parameter values of  $p_{th} = 1 \times 10^{-4}$ ,  $p_0 = 3 \times 10^{-9}$ , and  $t_p = 300$  ns, or better. This provides goals for the improvement in the device technologies necessary for quantum simulation. It should also be noted that these parameters are not completely independent and improvements in one of them may result in improvements in the others. For example, improving the physical failure probability may lead to better threshold failure probability by allowing some of the underlying operations to be weighted against one another. Similarly improving the threshold failure probability, may require choosing a more efficient quantum error correcting code which may have fundamentally shorter logical time.

#### IV. GENERALIZING TO HIGHER SPATIAL DIMENSIONS

The 1-D TIM ground state energy can be efficiently computed using classical computing resources by taking advantage of the linear geometry of the spin configuration and significantly reducing the effective state space to a polynomial in  $N$  [10]. A 2-D TIM with ferromagnetic and antiferromagnetic Ising couplings can be difficult to solve due to spin frustration. Many reductions to this problem still yield an exponential number of states with near degenerate energy [16]. As a result, the problem size scales exponentially with the size of the lattice. In contrast, the implementation of the quantum phase estimation circuit in Figure 1 is largely independent of the geometry of the  $N$  spin states and the values of  $\Gamma_i$  and  $J_{ij}$ , which suggests that it can be used for implementing efficiently higher-dimensional TIM problems. Consider, for example, the calculation of the ground state energy for the 2-D Villain's model [44] using the phase estimation circuit.

Villain's model is a 2-D square lattice Ising model with  $N^2$  spin sites in which the rows have all ferromagnetic coupling and the columns alternate between ferromagnetic and antiferromagnetic. Each of the  $N^2$  sites in Villain's model are represented by  $N^2$  qubits in a  $N \times N$  grid. The only change to the circuit for the phase estimation algorithm is the application of  $U_{zz}$  Ising interaction, which must be decomposed into two successive steps. First the rows of spin states are treated as the 1-D TIM problem in parallel, followed by the columns. Since the  $U_{zz}$  operations within each step are done in parallel, we still require  $N/2$  additional qubits for the cat-states. Given that the remaining operations, including the Quantum Fourier Transform implementation, remain the same, the increase in the number of time steps to implement an  $N^2$ -spin 2-D TIM problem, compared to the 1-D TIM problem, is by less than a factor of two. Similarly, the increase in the resource requirements between a 1-D and a 3-D TIM problem will be by less than a factor of three.

#### V. COMPARISON WITH FACTORING

Since the QLA architecture was initially evaluated in the context of Shor's quantum factoring algorithm [13], it would be interesting to consider how the resource requirements for implementing the TIM problem compare to those for implementing the factoring algorithm. In this section, we compare the implementation of the two applications on the QLA architecture and highlight some important differences between each application.

Even though both applications employ the phase estimation algorithm, there are several important differences. First, the precision requirements are different. For Shor's quantum factoring algorithm, the precision  $M$  must scale linearly with the size  $N$  of the  $N$ -bit number being factored [13], where  $N \geq 1024$  for mod-

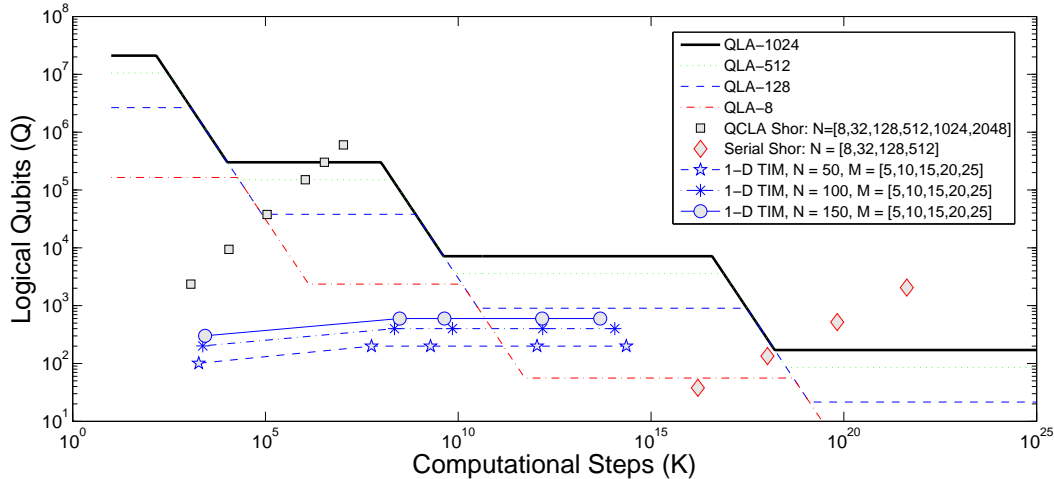


FIG. 8: (color online) Performance characteristics of different QLA-based quantum computers in KQ space with fixed amount of physical resources. The binary precision for the Ising problem of  $M = \{5, 10, 15, 20, 25\}$  corresponds to decimal precision of  $\{1, 3, 4, 6, 7\}$  digits, respectively.

ern cryptosystems. For quantum simulations, the desired precision is independent of the system size  $N$ , and the required  $M$  is small compared to factoring. The second difference lies in the implementation cost of the repeated powers of the controlled- $U(\tau)$  gates for each application. In Shor's algorithm, the gate is defined as  $U(\tau)|x\rangle = |ax \bmod N\rangle$ . Higher order powers of the unitary can be generated efficiently via modular exponentiation [13]. The result is that the implementation of  $U(2^m\tau)$  requires  $2m$  times the number of gates used for  $U(\tau)$ . For generic quantum simulation problems, the implementation cost of  $U(2^m\tau)$  equals  $2^m$  times  $U(\tau)$ , because of the Trotter parameter  $k$ . The implementation of the control unitary gates for quantum simulation is not as efficient as that for the modular exponentiation unitary gates. The third difference lies in the preparation of the initial  $N$ -qubit state  $|\Psi\rangle$ . The preparation of  $|\Psi\rangle$  for the TIM problem by adiabatic evolution is comparable in resource requirements to the phase estimation circuit. For Shor's quantum factoring algorithm  $|\Psi\rangle = |1\rangle$  in the computational basis and is easily prepared.

Finally, factoring integers large enough to be relevant for modern cryptanalysis requires several orders of magnitude more logical qubits than the scale of quantum simulation problems considered in this paper. At minimum, the factoring of an  $N$ -bit number requires  $2N + 3$  qubits, using the same one-control qubit circuit given in Figure 1 [45]. As shown later in this section, however, choosing to use only the minimum number of qubits required for factoring leads to very high error correction overhead. A more reasonable implementation of the factoring algorithm requires  $\mathcal{O}(N^2)$  number of logical qubits, which corresponds to millions of logical qubits for factoring a 1024-bit number. Quantum simulation problems require signif-

icantly less computational space and the problems considered in this paper require less than 500 logical qubits.

We examine how these differences affect the relative size of the QLA architecture required to implement each application. In particular, Figure 8 shows the performance of QLA-based quantum computers in KQ space with fixed physical resources. Each horizontal line corresponds to the KQ limit for a QLA-based architecture modeled for factoring a 1024-bit number (top-most horizontal dashed line), a 512-bit number, a 128-bit number, and an 8-bit number, respectively. The physical resources for each QLA- $N$  quantum computer (where  $N = \{1024, 512, 128, 8\}$  bits) are determined by how many logical qubits at level 2 error correction are required to implement the Quantum Carry Look-ahead Adder (QCLA) factoring circuit [12, 46], which requires  $\mathcal{O}(N^2)$  logical qubits and  $\mathcal{O}(N \log^2 N)$  logical cycles. The plateaus in each QLA- $N$  line of Figure 8 represent using all of the qubits at a specific level of encoding, with the top-most right-hand plateau representing level 1. Where the lines are sloped, the model is that only a certain number of the lower level encoded qubits can be used. Once this reaches the number of qubits that can be encoded at the next level, the quantum computer is switched from encoding level  $L$  to  $L + 1$  by using all the available level  $L$  qubits.

Figure 8 shows that a QLA- $N$  quantum computer is capable of executing an application using level  $L$  encoded qubits if the application instance is mapped *underneath* the line representing the computer at level  $L$ . Factoring a 1024-bit number, for example, falls directly on the level 2 portion of the QLA-1024 line (see the square markers). Anything above that line cannot be implemented with the QLA-1024 computer. Similarly, factoring a 128-bit number maps under the QLA-128 line, but can be accomplished using level 1 qubits. The TIM problem is mapped onto Figure 8 for  $N = 50, 100, 150$  and several binary precision instances:  $M = \{5, 10, 15, 20, 25\}$ . As expected, factoring requires many more logical qubits, however, both applications require similar levels of error correction. A decimal precision of up to 4 digits of accuracy ( $M = 15$ ) can be reached by using a quantum computer capable of factoring an 8-bit number at level 2 error correction, however higher precision quickly requires level 3 error correction.

The resources for implementing quantum factoring with one-control-qubit were calculated following the circuit in Figure 1, where the unitary gates are replaced with the unitary gates corresponding to modular exponentiation, as discussed in Reference [45]. The results are shown with the diamond-shaped markers in Figure 8. While this particular implementation is the least expensive factoring network in terms of logical qubits, the high precision requirement of  $M = O(N)$  makes this network very expensive in terms of time steps. In fact, the number of time steps required pushes the reliability requirements into level 4 error correction for factoring even modestly-sized numbers.

## VI. CONCLUSION

In this paper, the TIM quantum simulation circuit was decomposed into fault-tolerant operations and we estimated the circuit's resource requirements and number of logical cycles  $K$  as a function of the desired precision  $M$  in the estimate of the ground state energy. Our resource estimates were based on the QLA architecture and underlying technology parameters of trapped ions allowing us to estimate both  $K$ , as a function of the level of the error correction level, and the total length of the computation in real-time.

Our results indicate that even for small precision requirements  $K$  is large enough to require error correction. The growth of  $K$  is due to its linear dependence on the Trotter parameter  $k$ , which scales exponentially with the maximum desired precision  $M$ . In order for  $K$  to scale polynomially with the precision, new quantum simulation algorithms are required or systems must be chosen where the phase estimation algorithm can be implemented without the Trotter formula. The linear dependence of the number of time steps on  $k$  is due to the fact that  $U_x$  and the  $U_{zz}$  do not commute. However, there are some physical systems, whose Hamiltonians are composed of commuting terms, such as the nontransversal classical Ising model, which has a solution to the partition function in two dimensions but is NP-Complete for higher dimensions[47]. In those cases, Trotterization is unnecessary. In future work, we intend to generalize the calculations of the resource requirements to other physical systems and consider different ways to implement the phase estimation algorithm that limit its dependence on the Trotter formula.

- 
- [1] R. Feynman, International Journal of Theoretical Physics **21**, 467 (1982).
  - [2] S. Lloyd, Science **273**, 1073 (1996).
  - [3] D. Abrams and S. Lloyd, Phys. Rev. Lett. **79**, 2586 (1997).
  - [4] D. Abrams and S. Lloyd, Phys. Rev. Lett. **83**, 5162 (1999).
  - [5] C. Zalka, Proc. R. Soc. Lond. A **454**, 313 (1998).
  - [6] A. Aspuru-Guzik, A. Dutoi, P. Love, and M. Head-Gordon, Science **309**, 1704 (2005).
  - [7] I. Kassal, S. P. Jordan, P. J. Love, M. Mohseni, and A. Aspuru-Guzik, Proceedings of the National Academy of Science **105**, 1868 (2008).
  - [8] P. Pfeuty, Annals of Physics **57**, 79 (1970).
  - [9] S. Sachdev, *Quantum Phase Transitions* (Cambridge University Press, Cambridge, England, U.K., 1999).
  - [10] A. Juozapavicius, S. Caprara, and A. Rosengren, Phys. Rev. B **56**, 11097 (1997).
  - [11] A. Y. Kitaev, A. H. Shen, and M. N. Vyalyi, *Classical and Quantum Computation*, vol. 47 of *Graduate Studies in Mathematics* (American Mathematical Society, Providence, 2002).
  - [12] T. S. Metodi, D. D. Thaker, A. W. Cross, F. T. Chong, and I. L. Chuang, in *Proceedings of the 38th annual*

- IEEE/ACM International Symposium on Microarchitecture* (IEEE Computer Society, Washington, DC, 2005), pp. 305–318.
- [13] P. W. Shor, in *Proceedings of the 35th annual Symposium on Foundations of Computer Science* (IEEE, Los Alamitos, CA, 1994), pp. 124–134.
- [14] R. J. Elliott, P. Pfeuty, and C. Wood, *Phys. Rev. Lett.* **25**, 7 (1970).
- [15] R. Jullien, P. Pfeuty, J. N. Fields, and S. Doniach, *Phys. Rev. B* **18**, 3568 (1978).
- [16] R. Moessner and S. L. Sondhi, *Phys. Rev. B* **68**, 054405 (2003).
- [17] Y. Hu and A. Du, *J. Phys.:Condens. Matter* **20**, 125225 (2008).
- [18] M. Santos, *Phys. Rev. E* **61**, 7204 (2000).
- [19] S. Parker and M. Plenio, *Phys. Rev. Lett.* **85**, 3049 (2000).
- [20] R. Cleve, A. Ekert, C. Macchiavello, and M. Mosca, *Proc. R. Soc. Lon. A* **454**, 339 (1998).
- [21] K. R. Brown, R. J. Clark, and I. L. Chuang, *Phys. Rev. Lett.* **97**, 050504 (2006).
- [22] J. Kempe, A. Kitaev, and O. Regev, *SIAM Journal of Computing* **35**, 1070 (2006).
- [23] J. Biamonte and P. Love, *Phys. Rev. A* **78**, 012352 (2008).
- [24] M. Suzuki, *Phys. Lett. A* **165**, 387 (1992).
- [25] M. A. Nielsen and I. L. Chuang, *Quantum Computation and Quantum Information* (Cambridge University Press, Cambridge, UK, 2001).
- [26] C. M. Dawson and M. A. Nielsen, *Quant. Inf. Comp.* **6**, 81 (2005).
- [27] P. Shor, in *Proceedings of the 37th annual Symposium on the Foundations of Computer Science* (IEEE, Los Alamitos, CA, 1996), pp. 56–65.
- [28] D. Aharonov and M. Ben-Or, in *Proceedings of the 29th annual ACM Symposium on Theory of Computing* (ACM, New York, NY, USA, 1997), vol. 29, pp. 176–188.
- [29] A. Y. Kitaev, in *Proceedings of the 3rd International Conference of Quantum Communication and Measurement*, edited by O. Hirota, A. S. Holevo, and C. M. Caves (Plenum, New York, NY, 1997), pp. 181–188.
- [30] A. M. Steane, *Fortschritte der Physik* **46**, 443 (1999).
- [31] J. I. Cirac and P. Zoller, *Phys. Rev. Lett.* **74**, 4091 (1995).
- [32] D. Wineland, M. Barrett, J. Britton, J. Chiaverini, B. DeMarco, W. Itano, B. Jelenkovic, C. Langer, D. Leibfried, V. Meyer, et al., *Phil. Trans. R. Soc. Lond.* **A361**, 1349 (2003).
- [33] J. Chiaverini, R. B. Blakestad, J. Britton, J. D. Jost, C. Langer, D. Leibfried, R. Ozeri, and D. J. Wineland, *Quant. Info. Comput.* **5**, 419 (2005).
- [34] W. Dur, H. J. Briegel, J. I. Cirac, and P. Zoller, *Phys. Rev. A* **59**, 169 (1999).
- [35] A. M. Steane, *Phys. Rev. Lett.* **77**, 793 (1996).
- [36] T. M. Metodi, D. D. Thaker, and F. T. Chong, in *Proceedings of the 5th Workshop on Non-Silicon Computing (NSC-5)* (2007).
- [37] K. M. Svore, D. P. DiVincenzo, and B. M. Terhal, *Quant. Inf. Comp.* **7**, 297 (2007).
- [38] D. Gottesman, *Journal of Modern Optics* **47**, 333 (2000).
- [39] R. Ozeri, C. Langer, J. D. Jost, B. DeMarco, A. Ben-Kish, B. R. Blakestad, J. Britton, J. Chiaverini, W. M. Itano,

- D. B. Hume, et al., Phys. Rev. Lett. **95**, 030403 (2005).
- [40] S. Seidelin, J. Chiaverini, R. Reichle, J. J. Bollinger, D. Leibfried, J. Britton, J. H. Wesenberg, R. B. Blakestad, R. J. Epstein, D. B. Hume, et al., Phys. Rev. Lett. **96**, 253003 (2006).
- [41] R. Reichle, E. Knill, J. Britton, R. Blakestad, J. Jost, C. Langer, R. Ozeri, S. Seidelin, and D. Wineland, Nature **443**, 838 (2006).
- [42] A. M. Steane, Phys. Rev. A **68**, 042322 (2003).
- [43] P. Aliferis, D. Gottesman, and J. Preskill, Quant. Inf. Comp. **6**, 97 (2007).
- [44] R. Moessner and S. L. Sondhi, Phys. Rev. B **63**, 224401 (2001).
- [45] S. Beauregard, Quant. Inf. and Comp. **3**, 175 (2003).
- [46] R. V. Meter and K. M. Itoh, Phys. Rev. A **71**, 052320 (2005).
- [47] S. Istrail, in *Proceedings of the 32nd annual ACM Symposium on Theory of Computing* (ACM, New York, NY, 2000), p. 87.